World Journal of Gastroenterology

Submit a Manuscript: http://www.f6publishing.com

World J Gastroenterol 2018 August 7; 24(29): 3273-3280

DOI: 10.3748/wjg.v24.i29.3273

ISSN 1007-9327 (print) ISSN 2219-2840 (online)

ORIGINAL ARTICLE

Basic Study

High expression of type I inositol 1,4,5-trisphosphate receptor in the kidney of rats with hepatorenal syndrome

Jing-Bo Wang, Ye Gu, Ming-Xiang Zhang, Shun Yang, Yan Wang, Wei Wang, Xi-Ran Li, Yi-Tong Zhao, Hai-Tao Wang

Jing-Bo Wang, Ye Gu, Ming-Xiang Zhang, Yan Wang, Wei Wang, Xi-Ran Li, Yi-Tong Zhao, Liver Cirrhosis Ward, the Sixth People's Hospital of Shenyang, Shenyang 110006, Liaoning Province, China

Shun Yang, Liaoning Cancer Hospital & Institute, Shenyang 110042, Liaoning Province, China

Hai-Tao Wang, Department of General Surgery, the Second Affiliated Hospital of Shenyang Medical College, Shenyang 110002, Liaoning Province, China

ORCID number: Jing-Bo Wang (0000-0001-9207-6245); Ye Gu (0000-0002-3798-1119); Ming-Xiang Zhang (0000-0001-6519-3497); Shun Yang (0000-0003-4743-0588); Yan Wang (0000-0002-0427-3458); Wei Wang (0000-0002-4964-3280); Xi-Ran Li (0000-0002-3253-407X); Yi-Tong Zhao (0000-0002-5059-8608); Hai-Tao Wang (0000-0002-7385-0642).

Author contributions: Wang JB, Wang HT and Gu Y contributed equally to this work, and all of them were involved in the design and performing of the experiment, data analysis and drafting of the article; Zhang MX, Wang Y and Yang S participated in the study, hepatic and renal pathological examination and biochemical test; Li XR, Wang W and Zhao YT completed data analysis, Western blot analysis and real-time PCR and drafting of the paper.

Supported by Natural Science Foundation of Liaoning Province, No. 20170540826; Science and Technology Program of Shenyang City, No. 18-014-4-49; and Innovation Support Program of Shenyang City for Young and Middle-Aged Researchers, No. RC170051.

Institutional animal care and use committee statement: This study was approved by the Ethical Committee of the Sixth People's Hospital of Shenyang.

Conflict-of-interest statement: The authors declare no conflicts of interest.

Data sharing statement: No additional data are available.

Manuscript source: Unsolicited manuscript

Correspondence to: Hai-Tao Wang, MSc, Surgeon, Department of General Surgery, the Second Affiliated Hospital of Shenyang Medical College, No. 20, Beijiuma Road, Heping District, Shenyang 110002, Liaoning Province, China. whtszyypwk@163.com
Telephone: +86-18002452018
Fax: +86-24-31251510

Received: May 3, 2018
Peer-review started: May 4, 2018
First decision: June 6, 2018
Revised: June 19, 2018
Accepted: June 27, 2018
Article in press: June 27, 2018
Published online: August 7, 2018

Abstract

AIM

To detect the expression of type I inositol 1,4,5-trisphosphate receptor (IP_3RI) in the kidney of rats with hepatorenal syndrome (HRS).

METHODS

One hundred and twenty-five Sprague-Dawley rats were randomly divided into four groups to receive an intravenous injection of D-galactosamine (D-GalN) plus lipopolysaccharide (LPS; group G/L, n = 50), D-GalN alone (group G, n = 25), LPS alone (group L, n = 25), and normal saline (group NS, n = 25), respectively.

At 3, 6, 9, 12, and 24 h after injection, blood, liver, and kidney samples were collected. Hematoxylin-eosin staining of liver tissue was performed to assess hepatocyte necrosis. Electron microscopy was used to observe ultrastructural changes in the kidney. Western blot analysis and real-time PCR were performed to detect the expression of IP_3RI protein and mRNA in the kidney, respectively.

RESULTS

Hepatocyte necrosis was aggravated gradually, which was most significant at 12 h after treatment with D-galactosamine/lipopolysaccharide, and was characterized by massive hepatocyte necrosis. At the same time, serum levels of biochemical indicators including liver and kidney function indexes were all significantly changed. The structure of the renal glomerulus and tubules was normal at all time points. Western blot analysis indicated that IP_3RI protein expression began to rise at 3 h ($P < 0.05$) and peaked at 12 h ($P < 0.01$). Real-time PCR demonstrated that IP_3RI mRNA expression began to rise at 3 h ($P < 0.05$) and peaked at 9 h ($P < 0.01$).

CONCLUSION

IP_3RI protein expression is increased in the kidney of HRS rats, and may be regulated at the transcriptional level.

Key words: Hepatorenal syndrome; Type I inositol 1,4,5-trisphosphate receptor; Glomerular mesangial cells; Vascular smooth muscle cells

Core tip: Type I inositol 1,4,5-trisphosphate receptor (IP_3RI) protein expression is increased in the kidney of hepatorenal syndrome (HRS) rats, and IP_3RI protein expression may be regulated at the transcriptional level. Increased expression of IP_3RI may be closely associated with HRS development and progression through excessive renal vascular contraction resulting in insufficient renal blood perfusion.

Wang JB, Gu Y, Zhang MX, Yang S, Wang Y, Wang W, Li XR, Zhao YT, Wang HT. High expression of type I inositol 1,4,5-trisphosphate receptor in the kidney of rats with hepatorenal syndrome. *World J Gastroenterol* 2018; 24(29): 3273-3280 Available from: URL: http://www.wjgnet.com/1007-9327/full/v24/i29/3273.htm DOI: http://dx.doi.org/10.3748/wjg.v24.i29.3273

INTRODUCTION

Hepatorenal syndrome (HRS), one of the most severe complications of liver failure (LF) and the leading cause of death in LF[1], is functional renal failure secondary to LF[2-10]. At present, the exact pathogenesis of HRS is still unclear, and the reduction in renal blood flow induced by renal vasoconstriction is considered to play a central role in the development of HRS[11,12]. Renal blood flow is regulated by the contraction and relaxation of vascular smooth muscle cells (VSMCs) of glomerular afferent arteries and glomerular mesangial cells (GMCs), while the contraction and relaxation of VSMCs and GMCs are regulated by intracellular Ca^{2+} concentrations[13,14]. GMCs are in direct contact with glomerular endothelial cells. When GMCs contract, glomerular mesangial volume decreases by 20%-25%, glomerular capillary plexuses are reduced, and the area for glomerular filtration is reduced. Inositol 1,4,5-trisphosphate (IP_3) receptor (IP_3Rs) is the main Ca^{2+} release channel in cells. IP_3 is an intercellular second messenger mediating transmembrane signal transmission. When binding to IP_3Rs, IP_3 mediates intracellular calcium release and extracellular calcium influx[15,16]. VSMCs and GMCs transmit extracellular signals into the cell *via* the IP_3-IP_3R pathway, increasing intracellular Ca^{2+} concentrations[17,18]. Is high expression of renal IP_3Rs associated with HRS? To answer this question, in the present study we detected the expression of IP_3RI protein and mRNA in the kidney of HRS rats to determine the relationship between IP_3RI expression and HRS.

MATERIALS AND METHODS

Materials

Specific pathogen-free (SPF) Sprague-Dawley (SD) rats, weighing 220 g ± 20 g, were purchased from the Laboratory Animal Center of the Academy of Military Medical Sciences (Animal Certificate No. SCXK-2017-004; Beijing, China). Prior to experimentation, the rats were reared in separate cages at 23 ℃ ± 3 ℃ under a 12 h/12 h light/dark cycle, with free access to ordinary chow (purchased from the Laboratory Animal Center of China Medical University, Shenyang, China) and water. After one week of adaptation, the rats were used in the experiments.

D-galactosamine (D-GalN) and lipopolysaccharide (LPS) were purchased from Sigma (St. Louis, MO, United States). Anti-IP_3RI antibody was obtained from US Biological (St. Salem, OR, United States). An enhanced chemiluminescence (ECL) kit was purchased from Pierce, Dallas, TX, United States. RNAiso™ plus, Prime Script TM ᴿᵀ Reagent Kit, and SYBR® Premix EX Tag™ were purchased from TakaRa (Shiga, Japan).

Rat model of HRS

One hundred and twenty-five SD rats of SPF grade, weighing 220 ± 20 g, were randomly divided into four groups to receive an intravenous injection of D-GalN plus LPS (group G/L), D-GalN alone (group G), LPS alone (group L), and normal saline (group NS), respectively. Each group was further divided into five subgroups for testing at different time points (3, 6, 9,

12, and 24 h). Group G/L contained ten rats at each time point, and the other groups contained five rats at each time point. The rats were weighed and then injected with D-GalN (400 mg/kg body weight) and/or LPS (32 μg/kg) or NS (2 mL/kg) *via* the tail vein. Rats that died during the modeling process were excluded from the study. At 3, 6, 9, 12, and 24 h after modeling, the rats in groups G/L, G, and L were anesthetized with 0.8% pentobarbital sodium at 40 mg/kg *via* intraperitoneal injection and sacrificed to obtain liver and kidney tissues. A section of each tissue was fixed in formalin, and the remainder was preserved at -80 ℃ for Western blot and real-time PCR analysis of IP_3RI protein and mRNA expression, respectively.

Western blot analysis

For total protein preparation, renal tissue was lysed for 15 min in a lysis solution containing 50 mmol/L Tris-HCl (pH 7.4), 150 mmol/L NaCl, 1% Triton X-100, 1% sodium deoxycholate, 0.1% SDS, 1 mmol/L EDTA, 5 mg/mL leupeptin, sodium orthovanadate, sodium fluoride, and 1 mmol/L PMSF, and then centrifuged at 12000 rpm for 12 min. The supernatant was collected and preserved at -80 ℃.

After total protein concentration was determined using the bicinchoninic acid (BCA) method, the protein samples were mixed with 5 × loading buffer at a ratio of 4:1 (v/v), boiled for 5 min, resolved by 8% SDS-polyacrylamide gel electrophoresis, and transferred to polyvinylidene difluoride membranes. The membranes were then blocked with 5% skimmed milk, Tris-buffered saline and Tween-20, and incubated with primary antibody against IP_3RI (dilution, 1:1000) at 4 ℃ overnight. This was followed by incubation with horseradish peroxidase (HRP)-conjugated goat anti-rabbit secondary antibody (dilution, 1:3000) for 2 h at room temperature. The immunoblots were visualized using an enhanced chemiluminescence system. The molecular weight of the target band was 230 kDa. β-actin (45 kDa) was used as an internal control. Digital imaging software was used for densitometry analyses, and the relative IP_3RI level was calculated as IP_3RI grey value divided by β-actin grey value.

Real-time PCR

Total RNA was prepared from renal tissue using Trizol according to the manufacturer's instructions. After reverse transcription to cDNA in a 10-μL system containing 2.0 μL of 5 × Prime Script™ Buffer (for real time), 0.5 μL of Prime Script™ RT Enzyme Mi, 0.5 μL of Oligo dT Primer (50 μmol/L), 0.5 μL of Random 6-mers (100 μmol/L), 5.5 μL of RNase Free dH_2O, and 1.0 μL of RNA (500 ng/μL), real-time PCR was performed in a 25-μL system containing 12.5 μL of 2 × SYBR Premix Ex Tag™, 0.5 μL of PCR Forward Primer (10 μmol/L), 0.5 μL of PCR Reverse Primer (10 μmol/L), 9.5 μL of RNase Free dH_2O, and 2.0 μL of cDNA. Cycling parameters were 95 ℃ for 30 s and 45 cycles of 95 ℃ for 5 s, 57 ℃ for 20 s, and 72 ℃ for 30 s. Glyceraldehyde 3-phosphate dehydrogenase (GAPDH) was used as an endogenous reference. The primers used were as follows: forward, 5′-TCTGGCCAGCTGTCAGAACTAAAG-3′ and reverse, 5′-GTGGGTTGACATTCATGTGAGGA-3′ for IP_3RI, and forward, 5′-GACAACTTTGGCATCGTGGA-3′ and reverse, 5′-GACAACTTTGGCATCGTGGA-3′ for GAPDH. The double-standard curve method was used to determine the relative IP_3RI mRNA expression.

Statistical analysis

All statistical analyses were performed using SPSS 13.0 software. Numerical data, expressed as mean ± standard error of the mean, were compared using analysis of variance. P values < 0.05 were considered statistically significant.

RESULTS

Successful induction of HRS in rats with D-GalN/LPS

Following intravenous injection of D-GalN at 400 mg/kg body weight combined with LPS at 32 μg/kg in male SD rats, HRS was successfully induced. Twelve hours after injection, glomerular filtration rate (GFR) significantly decreased, liver and kidney function were severely impaired, and serum biochemical indices, such as alanine aminotransferase (ALT), blood urea nitrogen (BUN), and creatinine (Cr), exhibited significant changes. Hematoxylin-eosin staining showed massive hepatocyte necrosis with severe hemorrhage (Figure 1), while renal tissue had a normal morphology at the various time points (Figure 2). These changes were consistent with the clinical features of HRS.

Western blot analysis of IP_3RI protein expression

IP_3RI (230 kDa) and β-actin (45 kDa) were detected in all groups. Densitometry analyses showed that IP_3RI protein expression was significantly elevated in group G/L compared with group NS. This elevation began at 3 h (1.46 ± 0.07 *vs* 1.00 ± 0.05, P = 0.011), became obvious at 9 h, and reached a peak at 12 h (2.89 ± 0.14 *vs* 1.00 ± 0.05, P = 0.000) (Figure 3A).

At 12 h, the expression of IP_3RI protein in the kidney was significantly higher in group G/L than in groups G (1.17 ± 0.08) and L (1.02 ± 0.09) (P = 0.000 for both), thus excluding the impact of D-GalN or LPS on the expression of IP_3RI protein. There was no significant difference in IP_3RI protein expression between groups G and L (P = 0.245) or between group G or L and group NS (P > 0.05 for both) (Figure 3B).

RT-PCR analysis of IP_3RI mRNA expression

IP_3RI mRNA expression was significantly elevated in group G/L compared with group NS. This elevation began at 3 h (2.89 ± 0.51 *vs* 1.00 ± 0.00, P = 0.05), became obvious at 6 h (5.01 ± 0.38, P = 0.000), and reached a peak at 9 h (9.96 ± 0.63, P = 0.000). IP_3RI mRNA expression began to decline at 12 h, and at 24

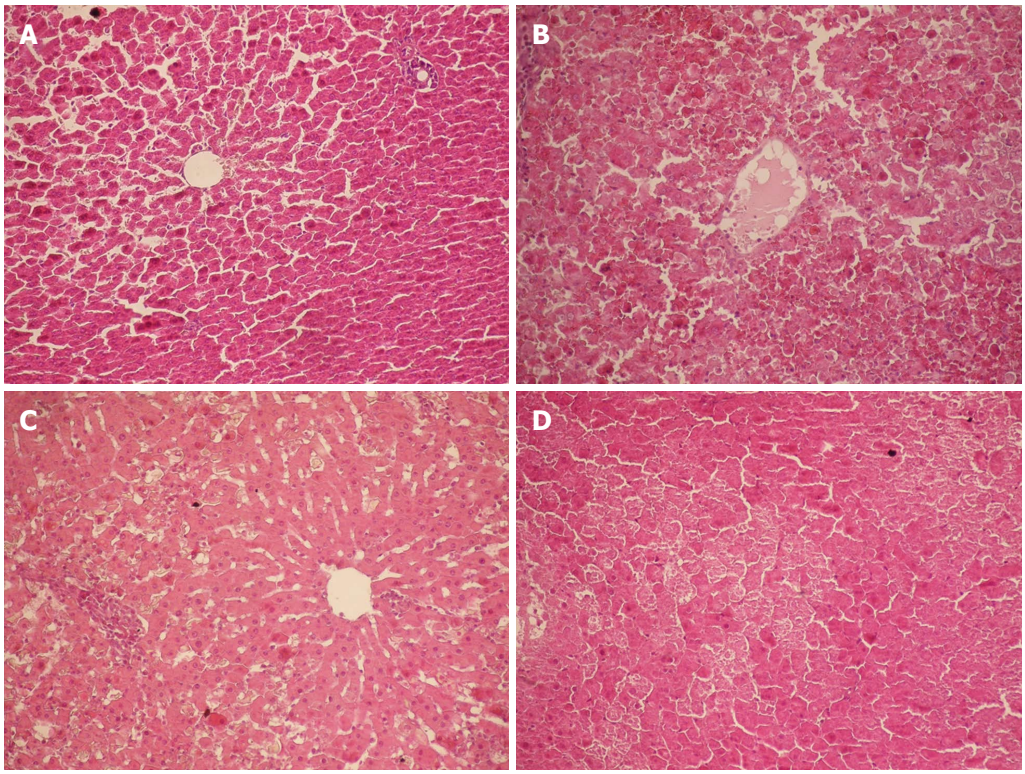

Figure 1 Histopathology of the liver (HE staining, × 200). A: Group Normal Saline (NS). Normal hepatocytes were arranged in cords; B: Group D-galactosamine (D-GalN) plus lipopolysaccharide (LPS) (G/L). At 12 h, massive hepatocyte necrosis with severe hemorrhage developed; C: Group D-GalN (G). At 12 h, spotty hepatocyte necrosis was observed; C: Group LPS (L). At 12 h, hepatocytes began to develop necrosis, with incomplete necrosis visible.

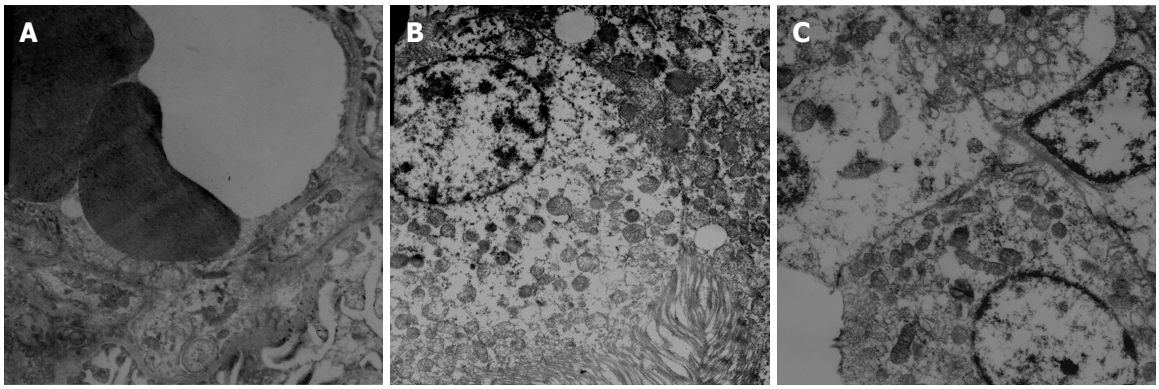

Figure 2 Histopathology of the kidney. A: The glomerular basement membrane of the kidney was intact, and the foot processes of podocytes and fenestra of endothelial cells were clearly visible; B: The basal part of proximal tubule cubical epithelial cells had abundant plasma membrane infolding, which was rich in longitudinally arranged mitochondria with intact cristae. On the free surface of proximal tubule cubical epithelial cells, microvilli were long and dense; C: The basal part of distal tubule cubical epithelial cells also had abundant plasma membrane infolding, which was rich in mitochondria. On the free surface of distal tubule cubical epithelial cells, microvilli were short and sparse.

h, it returned to the level observed at 6 h. IP_3RI mRNA expression at 9 h was significantly higher in group G/L than in groups G (1.43 ± 0.18) and L (1.29 ± 0.17) (P = 0.000 for both; Figure 4). IP_3RI mRNA expression did not differ significantly between group G or L and group NS (P > 0.05 for both).

DISCUSSION

HRS is one of the most common and severe complications of fulminant liver failure (FHF) and an advanced liver disease, with approximately 55% of FHF patients developing HRS[19,20]. The pathogenesis of HRS is still not completely clear, although it is believed to be associated with excessive renal vascular contraction, insufficient renal blood perfusion, sympathetic nervous system activation, and increased synthesis of vasoactive substances, all of which make the kidneys more sensitive to low perfusion[21,22]. Renal blood flow and GFR decrease significantly in HRS due to renal vasoconstriction, and many factors are involved in this process. A significant increase in vasocontracting factors

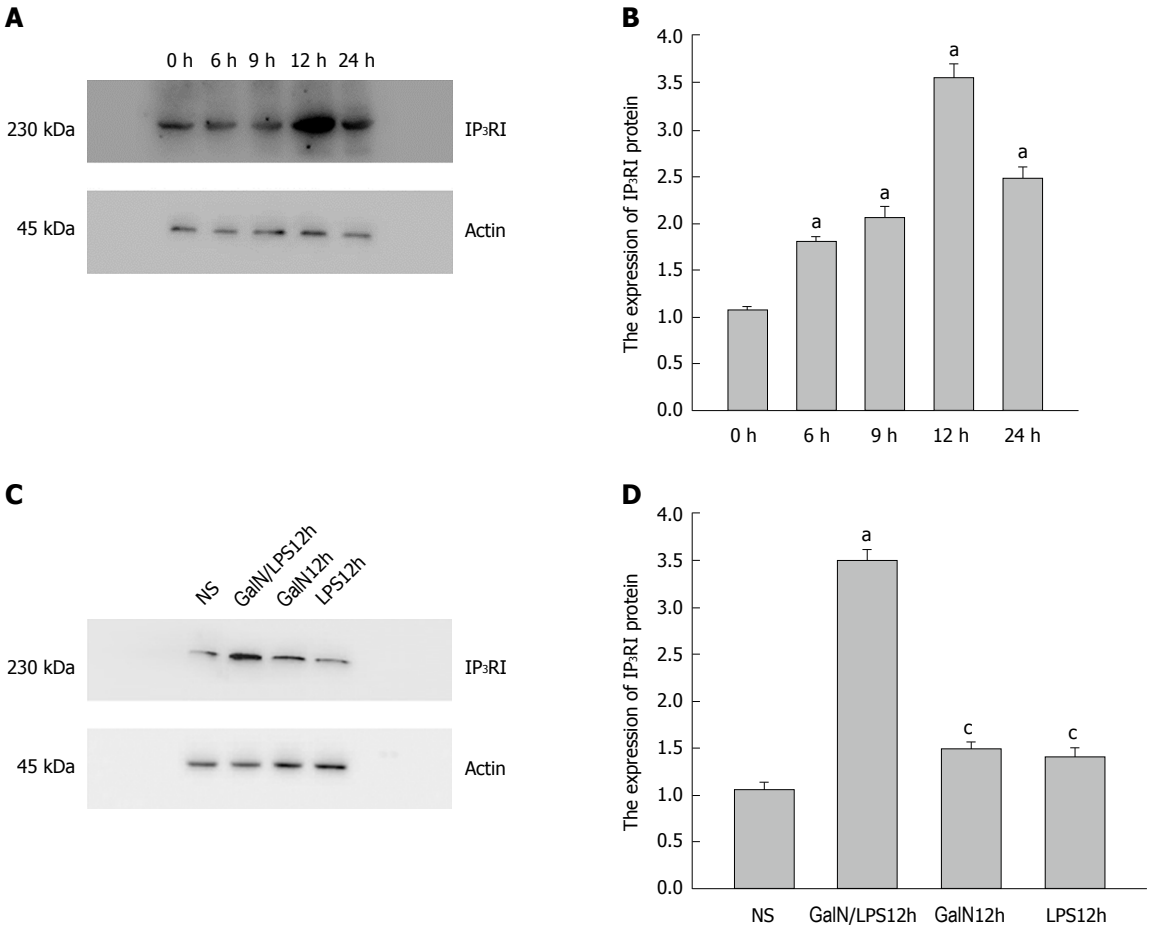

Figure 3 Expression of type Ⅰ inositol 1,4,5-trisphosphate receptor (IP_3RI) protein in the kidney of rats in each group. A: The expression of IP_3RI protein in the kidney significantly increased in group D-galactosamine (D-GalN) plus lipopolysaccharide (LPS) (G/L), and was especially prominent at 12 h [$^aP < 0.05$ *vs* group Normal Saline (NS)]. B: The expression of IP_3RI protein in the kidney significantly increased in group G/L compared with the other groups ($^aP < 0.05$ *vs* group NS, $^cP < 0.05$ *vs* group G/L).

[*e.g.*, endothelin (ET) and angiotensin II] in the blood not only leads to renal vascular contraction, but also decreases the glomerular filtration coefficient (K_f) and GFR[23,24]. The contraction of VSMCs results in reduced renal blood flow, while GMC contraction reduces the glomerular filtration fraction and coefficient. As both VSMCs and GMCs are extremely sensitive to vasoactive substances, GFR is significantly decreased in HRS. ET and angiotensin II are important renal vasocontracting factors, and they activate Ca^{2+} channels *via* the IP_3-IP_3Rs pathway. IP_3Rs is the intracellular calcium reservoir, which is present mainly in the endoplasmic reticulum and on the membrane, directly or indirectly mediating the calcium influx[25-27]. In addition, IP_3Rs is also present in the nucleus, participating in nuclear calcium release and regulating gene expression[28,29]. When IP_3 binds to IP_3Rs, a conformational change in IP_3Rs occurs, the calcium channel is open, and the calcium reserve in the endoplasmic reticulum is released into the cytoplasm. As a result, cytoplasmic free Ca^{2+} concentration ($[Ca^{2+}]_i$) increases, thus causing cell contraction[30-32]. Therefore, IP_3Rs mediates an important Ca^{2+} signaling pathway in the cell, and the expression of IP_3Rs is closely related to the sensitivity of the kidney to vasoconstrictors[33-35]. IP_3Rs has four types of ligand binding sites associated with calcium channels[36-39], and renal IP_3RI is mainly found in GMCs and VSMCs, and there is almost no IP_3RI on the surface of other renal cells[40,41]. Therefore, the expression levels of IP_3RI in renal GMCs and VSMCs may be related to renal vasoconstriction. As the opening of IP_3-IP_3Rs channels can increase intracellular $[Ca^{2+}]_i$, theoretically the expression level of IP_3RI is closely related to the intracellular $[Ca^{2+}]_i$ level. Wang *et al* observed increased expression of IP_3RI in the glomerular capillary loops and anterior artery of rats with liver cirrhosis by immunohistochemistry. However, it is unknown whether the expression of IP_3RI increases in FHF. To answer this question, we detected IP_3RI expression in the renal tissue of a rat model of FHF at different time points at both the protein and mRNA levels using Western blot and real-time quantitative PCR, respectively.

Semi-quantitative Western blot analysis demonstrated that IP_3RI protein expression was low in normal kidney tissue. Following treatment with D-GalN plus LPS, IP_3RI protein expression began to rise at 3 h and

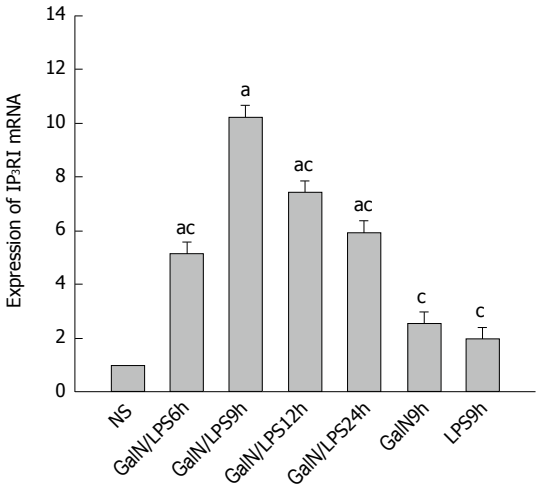

Figure 4 Expression of type Ⅰ inositol 1,4,5-trisphosphate receptor (IP_3RI) mRNA in the kidney of rats in group D-galactosamine (D-GalN) plus lipopolysaccharide (LPS) (G/L). The expression of IP_3RI mRNA in the kidney significantly increased in group G/L, and was especially prominent at 12 h ($^aP < 0.05$ *vs* group Normal Saline (NS), $^cP < 0.05$ *vs* group G/L).

reached a peak at 12 h. Interestingly, liver and kidney dysfunction and hepatocyte necrosis were most severe and blood TNF-α and ET-1 levels were highest at 12 h, which were concomitant with the elevation of IP_3RI protein expression in the kidney[42,43]. By treating the animals with D-GalN or LPS alone, we excluded the effect of these drugs on IP_3RI protein expression. As HRS developed 12 h after D-GalN/LPS administration, we compared the IP_3RI protein expression at this time point among the groups. The results showed that IP_3RI protein expression was high in group G/L and low in groups G, L, and NS.

In order to understand whether IP_3RI protein expression in the kidney is regulated at the transcriptional level, real-time quantitative PCR was performed. The fluorescent dye SYBR Green I[44,45] added to the PCR reaction system can be incorporated into double-stranded DNA with PCR amplification and markedly enhance fluorescence[46-48]. The relative expression levels of these two parameters were calculated by the housekeeping gene GAPDH. It was found that the relative expression of IP_3RI mRNA to GAPDH mRNA began to rise 3 h after D-GalN and LPS administration, but the protein level did not rise at this time point. At 9 h, the expression level of IP_3RI mRNA reached the highest level. Although the protein level was also high at this time point, it was lower than that at 12 h. The expression of IP_3RI mRNA began to decrease, but it was still significantly higher than that in the control group. These changes can be explained from two aspects. On the one hand, IP_3RI mRNA expression may be prior to protein expression, which is associated not only with the translation efficiency and the speed of mRNA degradation, but also with the rate of protein degradation. On the other hand, the protein synthesis process also includes the assembly and translocation of proteins in ribosomes, which may affect the final expression of IP_3RI protein.

In conclusion, joint D-GalN/LPS administration can induce HRS in SD rats at 12 h, which is concomitant with peak IP_3RI protein expression in the kidney. Increased IP_3RI protein expression may be regulated at the transcriptional level. Thus, increased expression of IP_3RI may be closely associated with HRS development and progression.

ARTICLE HIGHLIGHTS

Research background

Hepatorenal syndrome (HRS) is one of the common and severe complications of liver failure and advanced liver disease, with approximately 55% of these patients developing this severe complication. At present, HRS has unclear pathogenesis, limited treatment options, and poor therapeutic efficacy. Once renal dysfunction aggravates rapidly, 60%-80% of patients with HRS will die. Therefore, elucidating the mechanism underlying the development and progression of HRS and taking effective preventive and therapeutic measures may improve the success rate of rescue, the incidence rate, and the mortality rate of HRS.

Research motivation

To detect the protein and mRNA expression of type Ⅰ inositol 1,4,5-trisphosphate receptor (IP_3RI) in the kidney of rats with HRS by Western blot and real-time PCR.

Research objectives

To explore whether high expression of renal IP_3RI is associated with Ca^{2+} influx in vascular smooth muscle cells of glomerular afferent arteries and glomerular mesangial cells in rats with HRS.

Research methods

D-galactosamine (D-GalN) and/or lipopolysaccharide (LPS) were used to treat male Sprague-Dawley (SD) rats *via* the tail vein. Twelve hours after injection, massive hepatocyte necrosis with severe hemorrhage occurred in the liver, while renal tissue had a normal morphology. In addition, liver and kidney function was impaired severely, and serum biochemical indexes exhibited significant changes. These changes were consistent with the clinical features of HRS. Western blot and real-time PCR were then used to detect the protein and mRNA expression of renal IP_3RI, respectively.

Research results

IP_3RI protein expression was significantly elevated in rats with HRS. The elevation began at 3 h and reached the peak at 12 h. IP_3RI mRNA expression was also significantly elevated in rats with HRS. The elevation began at 3 h and peaked at 9 h.

Research conclusions

Joint D-GalN/LPS administration can induce HRS in SD rats at 12 h, which is concomitant with peaked IP_3RI protein and mRNA expression in the kidney. Increased expression of IP_3RI may be closely associated with HRS development and progression.

Research perspectives

Our results suggest that IP_3RI may be a signal molecule involved in the reduction of renal blood flow induced by renal vasoconstriction in HRS, thus providing a theoretical basis for further research of the pathogenesis of HRS. Gene silencing technology may be adopted to further elucidate the role of IP_3RI in the pathogenesis of HRS.

REFERENCES

1 **Hernaez R**, Solà E, Moreau R, Ginès P. Acute-on-chronic liver failure: an update. *Gut* 2017; **66**: 541-553 [PMID: 28053053 DOI:

10.1136/gutjnl-2016-312670]
2 **de Mattos ÁZ**, de Mattos AA, Méndez-Sánchez N. Hepatorenal syndrome: Current concepts related to diagnosis and management. *Ann Hepatol* 2016; **15**: 474-481 [PMID: 27236146]
3 **Bittencourt PL**, Farias AQ, Terra C. Renal failure in cirrhosis: Emerging concepts. *World J Hepatol* 2015; **7**: 2336-2343 [PMID: 26413223 DOI: 10.4254/wjh.v7.i21.2336]
4 **Khan MQ**, Anand V, Hessefort N, Hassan A, Ahsan A, Sonnenberg A, Fimmel CJ. Utility of Electronic Medical record-based Fibrosis Scores in Predicting Advanced Cirrhosis in Patients with Hepatitic C Virus Infection. *J Transl Int Med* 2017; **5**: 43-48 [PMID: 28680838 DOI: 10.1515/jtim-2017-0011]
5 **Torres-Valadez R**, Roman S, Jose-Abrego A, Sepulveda-Villegas M, Ojeda-Granados C, Rivera-Iñiguez I, Panduro A. Early Detection of Liver Damage in Mexican Patients with Chronic Liver Disease. *J Transl Int Med* 2017; **5**: 49-57 [PMID: 28680839 DOI: 10.1515/jtim-2017-0003]
6 **Abenavoli L**, Milic N, Luzza F, Boccuto L, De Lorenzo A. Polyphenols Treatment in Patients with Nonalcoholic Fatty Liver Disease. *J Transl Int Med* 2017; **5**: 144-147 [PMID: 29164049 DOI: 10.1515/jtim-2017-0027]
7 **Elbahrawy A**, Elwassief A, Abdallah AM, Kasem A, Mostafa S, Makboul K, Ali MS, Alashker A, Eliwa AM, Shahbah H, Othman MA, Morsy MH, Abdelbaseer MA, Abdelhafeez H. Hepatitis C Virus Exposure Rate among Health-care Workers in Rural Lower Egypt Governorates. *J Transl Int Med* 2017; **5**: 164-168 [PMID: 29085789 DOI: 10.1515/jtim-2017-0024]
8 **Das UN**. Renin-angiotensin-aldosterone system in insulin resistance and metabolic syndrome. *J Transl Int Med* 2016; **4**: 66-72 [PMID: 28191524 DOI: 10.1515/jtim-2016-0022]
9 **Bao H**, Peng A. The Green Tea Polyphenol(-)-epigallocatechin-3-gallate and its beneficial roles in chronic kidney disease. *J Transl Int Med* 2016; **4**: 99-103 [PMID: 28191529 DOI: 10.1515/jtim-2016-0031]
10 **Wang L**, Mohan C. Contrast-enhanced ultrasound: A promising method for renal microvascular perfusion evaluation. *J Transl Int Med* 2016; **4**: 104-108 [PMID: 28191530 DOI: 10.1515/jtim-2016-0033]
11 **Dundar HZ**, Yılmazlar T. Management of hepatorenal syndrome. *World J Nephrol* 2015; **4**: 277-286 [PMID: 25949942 DOI: 10.5527/wjn.v4.i2.277]
12 **Colle I**, Laterre PF. Hepatorenal syndrome: the clinical impact of vasoactive therapy. *Expert Rev Gastroenterol Hepatol* 2018; **12**: 173-188 [PMID: 29258378 DOI: 10.1080/17474124.2018.1417034]
13 **Geyer M**, Huang F, Sun Y, Vogel SM, Malik AB, Taylor CW, Komarova YA. Microtubule-Associated Protein EB3 Regulates IP3 Receptor Clustering and Ca(2+) Signaling in Endothelial Cells. *Cell Rep* 2015; **12**: 79-89 [PMID: 26119739 DOI: 10.1016/j.celrep.2015.06.001]
14 **Taylor CW**, Tovey SC, Rossi AM, Lopez Sanjurjo CI, Prole DL, Rahman T. Structural organization of signalling to and from IP3 receptors. *Biochem Soc Trans* 2014; **42**: 63-70 [PMID: 24450629 DOI: 10.1042/BST20130205]
15 **Chandrasekhar R**, Alzayady KJ, Yule DI. Using concatenated subunits to investigate the functional consequences of heterotetrameric inositol 1,4,5-trisphosphate receptors. *Biochem Soc Trans* 2015; **43**: 364-370 [PMID: 26009177 DOI: 10.1042/BST20140287]
16 **Alzayady KJ**, Wang L, Chandrasekhar R, Wagner LE 2nd, Van Petegem F, Yule DI. Defining the stoichiometry of inositol 1,4,5-trisphosphate binding required to initiate Ca2+ release. *Sci Signal* 2016; **9**: ra35 [PMID: 27048566 DOI: 10.1126/scisignal.aad6281]
17 **Ambudkar IS**. Ca^{2+} signaling and regulation of fluid secretion in salivary gland acinar cells. *Cell Calcium* 2014; **55**: 297-305 [PMID: 24646566 DOI: 10.1016/j.ceca.2014.02.009]
18 **Provence A**, Rovner ES, Petkov GV. Regulation of transient receptor potential melastatin 4 channel by sarcoplasmic reticulum inositol trisphosphate receptors: Role in human detrusor smooth muscle function. *Channels* (Austin) 2017; **11**: 459-466 [PMID: 28644055 DOI: 10.1080/19336950.2017.1341023]
19 **Bajaj JS**, O'Leary JG, Reddy KR, Wong F, Biggins SW, Patton H, Fallon MB, Garcia-Tsao G, Maliakkal B, Malik R, Subramanian RM, Thacker LR, Kamath PS; North American Consortium For The Study Of End-Stage Liver Disease (NACSELD). Survival in infection-related acute-on-chronic liver failure is defined by extrahepatic organ failures. *Hepatology* 2014; **60**: 250-256 [PMID: 24677131 DOI: 10.1002/hep.27077]
20 **Lenz K**, Buder R, Kapun L, Voglmayr M. Treatment and management of ascites and hepatorenal syndrome: an update. *Therap Adv Gastroenterol* 2015; **8**: 83-100 [PMID: 25729433 DOI: 10.1177/1756283X14564673]
21 **Piano S**, Schmidt HH, Ariza X, Amoros A, Romano A, Hüsing-Kabar A, Solà E, Gerbes A, Bernardi M, Alessandria C, Scheiner B, Tonon M, Maschmeier M, Solè C, Trebicka J, Gustot T, Nevens F, Arroyo V, Gines P, Angeli P; EASL CLIF Consortium, European Foundation for the Study of Chronic Liver Failure (EF Clif). Association Between Grade of Acute on Chronic Liver Failure and Response to Terlipressin and Albumin in Patients With Hepatorenal Syndrome. *Clin Gastroenterol Hepatol* 2018; Epub ahead of print [PMID: 29391267 DOI: 10.1016/j.cgh.2018.01.035]
22 **Tsien CD**, Rabie R, Wong F. Acute kidney injury in decompensated cirrhosis. *Gut* 2013; **62**: 131-137 [PMID: 22637695 DOI: 10.1136/gutjnl-2011-301255]
23 **Bekpinar S**, Vardagli D, Unlucerci Y, Can A, Uysal M, Gurdol F. Effect of rosiglitazone on asymmetric dimethylarginine metabolism in thioacetamide-induced acute liver injury. *Pathophysiology* 2015; **22**: 153-157 [PMID: 26224212 DOI: 10.1016/j.pathophys.2015.06.003]
24 **Sridharan K**, Sivaramakrishnan G. Vasoactive Agents for Hepatorenal Syndrome: A Mixed Treatment Comparison Network Meta-Analysis and Trial Sequential Analysis of Randomized Clinical Trials. *J Gen Intern Med* 2018; **33**: 97-102 [PMID: 28924736 DOI: 10.1007/s11606-017-4178-8]
25 **Ullah G**, Ullah A. Mode switching of Inositol 1,4,5-trisphosphate receptor channel shapes the Spatiotemporal scales of Ca2+ signals. *J Biol Phys* 2016; **42**: 507-524 [PMID: 27154029 DOI: 10.1007/s10867-016-9419-2]
26 **Alzayady KJ**, Sebé-Pedrós A, Chandrasekhar R, Wang L, Ruiz-Trillo I, Yule DI. Tracing the Evolutionary History of Inositol, 1, 4, 5-Trisphosphate Receptor: Insights from Analyses of Capsaspora owczarzaki Ca2+ Release Channel Orthologs. *Mol Biol Evol* 2015; **32**: 2236-2253 [PMID: 25911230 DOI: 10.1093/molbev/msv098]
27 **Bánsághi S**, Golenár T, Madesh M, Csordás G, RamachandraRao S, Sharma K, Yule DI, Joseph SK, Hajnóczky G. Isoform- and species-specific control of inositol 1,4,5-trisphosphate (IP3) receptors by reactive oxygen species. *J Biol Chem* 2014; **289**: 8170-8181 [PMID: 24469450 DOI: 10.1074/jbc.M113.504159]
28 **Okeke E**, Parker T, Dingsdale H, Concannon M, Awais M, Voronina S, Molgó J, Begg M, Metcalf D, Knight AE, Sutton R, Haynes L, Tepikin AV. Epithelial-mesenchymal transition, IP3 receptors and ER-PM junctions: translocation of Ca2+ signalling complexes and regulation of migration. *Biochem J* 2016; **473**: 757-767 [PMID: 26759379 DOI: 10.1042/BJ20150364]
29 **Subedi KP**, Son MJ, Chidipi B, Kim SW, Wang J, Kim KH, Woo SH, Kim JC. Signaling Pathway for Endothelin-1- and Phenylephrine-Induced cAMP Response Element Binding Protein Activation in Rat Ventricular Myocytes: Role of Inositol 1,4,5-Trisphosphate Receptors and CaMKII. *Cell Physiol Biochem* 2017; **41**: 399-412 [PMID: 28214885 DOI: 10.1159/000456422]
30 **Fan G**, Baker ML, Wang Z, Baker MR, Sinyagovskiy PA, Chiu W, Ludtke SJ, Serysheva II. Gating machinery of InsP3R channels revealed by electron cryomicroscopy. *Nature* 2015; **527**: 336-341 [PMID: 26458101 DOI: 10.1038/nature15249]
31 **Seo MD**, Velamakanni S, Ishiyama N, Stathopulos PB, Rossi AM, Khan SA, Dale P, Li C, Ames JB, Ikura M, Taylor CW. Structural and functional conservation of key domains in InsP3 and ryanodine receptors. *Nature* 2012; **483**: 108-112 [PMID: 22286060 DOI: 10.1038/nature10751]

32 **Alzayady KJ**, Wagner LE 2nd, Chandrasekhar R, Monteagudo A, Godiska R, Tall GG, Joseph SK, Yule DI. Functional inositol 1,4,5-trisphosphate receptors assembled from concatenated homo- and heteromeric subunits. *J Biol Chem* 2013; **288**: 29772-29784 [PMID: 23955339 DOI: 10.1074/jbc.M113.502203]

33 **Cao P**, Falcke M, Sneyd J. Mapping Interpuff Interval Distribution to the Properties of Inositol Trisphosphate Receptors. *Biophys J* 2017; **112**: 2138-2146 [PMID: 28538151 DOI: 10.1016/j.bpj.2017.03.019]

34 **Chandrasekhar R**, Alzayady KJ, Wagner LE 2nd, Yule DI. Unique Regulatory Properties of Heterotetrameric Inositol 1,4,5-Trisphosphate Receptors Revealed by Studying Concatenated Receptor Constructs. *J Biol Chem* 2016; **291**: 4846-4860 [PMID: 26755721 DOI: 10.1074/jbc.M115.705301]

35 **Yang J**, Vais H, Gu W, Foskett JK. Biphasic regulation of InsP3 receptor gating by dual Ca2+ release channel BH3-like domains mediates Bcl-xL control of cell viability. *Proc Natl Acad Sci USA* 2016; **113**: E1953-E1962 [PMID: 26976600 DOI: 10.1073/pnas.1517935113]

36 **Sun MY**, Geyer M, Komarova YA. IP_3 receptor signaling and endothelial barrier function. *Cell Mol Life Sci* 2017; **74**: 4189-4207 [PMID: 28803370 DOI: 10.1007/s00018-017-2624-8]

37 **Golebiewska U**, Kay JG, Masters T, Grinstein S, Im W, Pastor RW, Scarlata S, McLaughlin S. Evidence for a fence that impedes the diffusion of phosphatidylinositol 4,5-bisphosphate out of the forming phagosomes of macrophages. *Mol Biol Cell* 2011; **22**: 3498-3507 [PMID: 21795401 DOI: 10.1091/mbc.E11-02-0114]

38 **Gulyás G**, Tóth JT, Tóth DJ, Kurucz I, Hunyady L, Balla T, Várnai P. Measurement of inositol 1,4,5-trisphosphate in living cells using an improved set of resonance energy transfer-based biosensors. *PLoS One* 2015; **10**: e0125601 [PMID: 25932648 DOI: 10.1371/journal.pone.0125601]

39 **Takeda Y**, Shimayoshi T, Holz GG, Noma A. Modeling analysis of inositol 1,4,5-trisphosphate receptor-mediated Ca2+ mobilization under the control of glucagon-like peptide-1 in mouse pancreatic β-cells. *Am J Physiol Cell Physiol* 2016; **310**: C337-C347 [PMID: 26741144 DOI: 10.1152/ajpcell.00234.2015]

40 **Bojjireddy N**, Botyanszki J, Hammond G, Creech D, Peterson R, Kemp DC, Snead M, Brown R, Morrison A, Wilson S, Harrison S, Moore C, Balla T. Pharmacological and genetic targeting of the PI4KA enzyme reveals its important role in maintaining plasma membrane phosphatidylinositol 4-phosphate and phosphatidylinositol 4,5-bisphosphate levels. *J Biol Chem* 2014; **289**: 6120-6132 [PMID: 24415756 DOI: 10.1074/jbc.M113.531426]

41 **Wagner LE 2nd**, Yule DI. Differential regulation of the $InsP_3$ receptor type-1 and -2 single channel properties by $InsP_3$, Ca^{2+} and ATP. *J Physiol* 2012; **590**: 3245-3259 [PMID: 22547632 DOI: 10.1113/jphysiol.2012.228320]

42 **Wang JB**, Wang DL, Wang HT, Wang ZH, Wen Y, Sun CM, Zhao YT, Wu J, Liu P. Tumor necrosis factor-alpha-induced reduction of glomerular filtration rate in rats with fulminant hepatic failure. *Lab Invest* 2014; **94**: 740-751 [PMID: 24887412 DOI: 10.1038/labinvest.2014.71]

43 **Wang JB**, Wang HT, Li LP, Yan YC, Wang W, Liu JY, Zhao YT, Gao WS, Zhang MX. Development of a rat model of D-galactosamine/lipopolysaccharide induced hepatorenal syndrome. *World J Gastroenterol* 2015; **21**: 9927-9935 [PMID: 26379397 DOI: 10.3748/wjg.v21.i34.9927]

44 **Barbau-Piednoir E**, Bertrand S, Mahillon J, Roosens NH, Botteldoorn N. SYBR®Green qPCR Salmonella detection system allowing discrimination at the genus, species and subspecies levels. *Appl Microbiol Biotechnol* 2013; **97**: 9811-9824 [PMID: 24113820 DOI: 10.1007/s00253-013-5234-x]

45 **Barbau-Piednoir E**, Denayer S, Botteldoorn N, Dierick K, De Keersmaecker SCJ, Roosens NH. Detection and discrimination of five E. coli pathotypes using a combinatory SYBR® Green qPCR screening system. *Appl Microbiol Biotechnol* 2018; **102**: 3267-3285 [PMID: 29460001 DOI: 10.1007/s00253-018-8820-0]

46 **Barbau-Piednoir E**, Botteldoorn N, Mahillon J, Dierick K, Roosens NH. Fast and discriminative CoSYPS detection system of viable Salmonella spp. and Listeria spp. in carcass swab samples. *Int J Food Microbiol* 2015; **192**: 103-110 [PMID: 25440553 DOI: 10.1016/j.ijfoodmicro.2014.09.018]

47 **Acevedo AM**, Perera CL, Vega A, Ríos L, Coronado L, Relova D, Frías MT, Ganges L, Núñez JI, Pérez LJ. A duplex SYBR Green I-based real-time RT-PCR assay for the simultaneous detection and differentiation of Massachusetts and non-Massachusetts serotypes of infectious bronchitis virus. *Mol Cell Probes* 2013; **27**: 184-192 [PMID: 23810983 DOI: 10.1016/j.mcp.2013.06.001]

48 **Fellahi S**, El Harrak M, Kuhn JH, Sebbar G, Bouaiti el A, Khataby K, Fihri OF, El Houadfi M, Ennaji MM. Comparison of SYBR green I real-time RT-PCR with conventional agarose gel-based RT-PCR for the diagnosis of infectious bronchitis virus infection in chickens in Morocco. *BMC Res Notes* 2016; **9**: 231 [PMID: 27106608 DOI: 10.1186/s13104-016-2037-z]

P- Reviewer: Jarcuska P, Markic D **S- Editor**: Gong ZM
L- Editor: Filipodia **E- Editor**: Huang Y

Published by **Baishideng Publishing Group Inc**
7901 Stoneridge Drive, Suite 501, Pleasanton, CA 94588, USA
Telephone: +1-925-223-8242
Fax: +1-925-223-8243
E-mail: bpgoffice@wjgnet.com
Help Desk: http://www.f6publishing.com/helpdesk
http://www.wjgnet.com

ISSN 1007-9327